High-magnetic-field thermal-conductivity measurements in graphite intercalation compounds

J. Heremans
Laboratoire de Physico-Chimie et de Physique de l'État Solide, Place Croix du Sud, 1, B-1348 Louvain-la-Neuve, Belgium
and Center for Materials Science and Engineering, Massachusetts Institute of Technology, Cambridge, Massachusetts 02139

M. Shayegan and M. S. Dresselhaus
Department of Electrical Engineering and Computer Science and Center for Materials Science and Engineering, Massachusetts Institute of Technology, Cambridge, Massachusetts 02139

J-P. Issi
Laboratoire de Physico-Chimie et de Physique de l'État Solide, Place Croix du Sud, 1, B-1348 Louvain-la-Neuve, Belgium
(Received 18 December 1981)

The thermal conductivity of donor and acceptor graphite intercalation compounds is studied at high magnetic fields in order to separate the electronic from the lattice contribution. Measurements are reported in fields up to 15 T at temperatures from 2 to 50 K. For one dilute sample of both a donor and an acceptor compound, the electronic and lattice contributions to the thermal conductivity are separated over almost the entire temperature range up to 50 K. The temperature dependence of the electronic and lattice contributions is discussed qualitatively.

I. INTRODUCTION

The thermal conductivity, κ, of graphite intercalation compounds (GIC's) has been measured as a function of temperature on bromine-intercalated polycrystalline graphite[1] in the range $100 < T < 300$ K, and very recently on $FeCl_3$ and potassium-intercalated highly oriented pyrolytic graphite[2-4] (HOPG) for $2 < T < 300$ K. The latter results pertain to both c-axis and in-plane measurements. Even though the phonon spectra are very similar in graphite and GIC's, the temperature dependence of κ in GIC's is drastically different from that of pristine graphite.

Below room temperature, two mechanisms contribute to heat conduction in a solid: the lattice and the charge carriers: electrons or holes. It is usually assumed that these mechanisms do not strongly interact with each other, and hence the lattice and the charge carriers act like conductors in parallel and the total thermal conductivity κ is given by

$$\kappa = \kappa_L + \kappa_E \ , \tag{1}$$

where κ_L is the lattice contribution and κ_E the electronic contribution to the thermal conductivity.

In pure graphite, κ_L is dominant for $T > 3$ K. The temperature dependence of the thermal conductivity then displays a $T^{2.3}$-to- $T^{2.6}$ law up to liquid-nitrogen temperatures. At higher temperatures, the more perfect (crystallographically) graphite samples show a maximum in κ for $T > 100$ K, above which κ decreases due to umklapp phonon-phonon scattering.[5] In samples of poorer quality, [6,7] the maximum in κ shifts to higher temperatures and has a smaller magnitude.

In all GIC samples, κ around room temperature displays a broad maximum (or a plateau), which has therefore been attributed to lattice conduction.[2-4] Below ~ 10 K, most GIC's display a linear T^1 dependence of κ, quite unlike graphite. It has been assumed until now, by comparison with κ in other semimetals,[8] that this linear behavior is due to a dominant electronic thermal conductivity. The aim of the present work is to prove this assumption experimentally and to examine in detail the electronic term and its relationship to the electrical conductivity.

In the domain of elastic scattering of the charge carriers, κ_E is directly proportional to the electrical conductivity via the Wiedemann-Franz relation

$$\kappa_E = L_0 \sigma T \,, \tag{2}$$

where L_0 (2.44×10^{-8} V^2K^{-2}) is the free-electron Lorenz number. Equation (2) implies that if we apply a magnetic field to a sample with high magnetoresistance, κ_E will decrease. In a solid where κ_L and κ_E represent competitive conduction mechanisms, a magnetic field will deplete κ_E so that eventually κ_L becomes dominant. In the present analysis we assume that κ_L is field independent and that κ_E can be computed from Eq. (1).

This separation of the thermal conductivity has been attempted in other materials,[9] including bismuth[10] and graphite[11] below 3 K. Unlike the two latter semimetals, GIC's have lower carrier mobilities, so that high magnetic fields are required to achieve separation between κ_E and κ_L. The problems associated with the use of high magnetic fields and small samples are discussed in Sec. II, which deals with experimental techniques. In Sec. III we present the experimental results and describe their characteristic features. Finally, in the discussion (Sec. IV), we draw some qualitative conclusions about the scattering mechanisms for phonons and electrons in graphite intercalation compounds.

II. EXPERIMENTAL SETUP

Thermal-conductivity measurements are traditionally carried out by passing a heat flow through a sample to a heat sink held at constant temperature. To make quantitative measurements, all the heat must flow through the sample. Graphite and its intercalation compounds have sufficiently high thermal conductivity so that even though the samples are thin ($\sim$2 mm), heat losses may be reduced to an insignificant level by use of the sample geometry shown in Fig. 1. Magnetic fields along the c axis are obtained using a Bitter magnet.

Technically, two specific problems had to be solved to carry out the measurements reported here. The problems are due to the small size of available samples, and to the presence of a large magnetic field. Additional difficulties arise from the ripple ($\sim$2%) in the magnetic field.

When no magnetic field is applied, the thermal conductivity of such small and fragile samples is measured by means of thermocouples.[12] In a Bitter magnet, the field dependence and electromagnetically induced noise makes the use of thermocouples impractical. On the other hand, carbon-glass resistor thermometers have been recently calibrated in fields up to 20 T, by Sample *et al.*[13] Two sensors from the same manufacturer as were used by these authors[13] proved adequate for these experiments. These two sensors were especially chosen to have very similar resistances at 4.2 K. The difference in magnetoresistance between the two sensors was within the experimental error of the calibration of the sensors in a magnetic field.

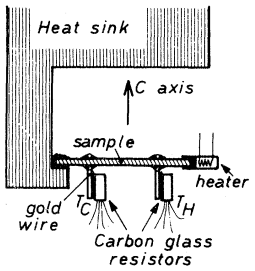

FIG. 1. Schematic representation of the experimental setup: A heater and sink method, using carbon-glass resistors as the temperature probes. Magnetic field provided by a Bitter magnet is applied along the c axis of the sample.

Figure 1 shows the schematic setup for the classical heater and sink thermal-conductivity measurement, which was used in the present work. The sample was attached to a heat sink by means of GE7031 varnish. The heater consisted of a strain gauge mounted on a small gold clamp that was squeezed on to the end of the sample and varnished again. The electrical contacts to the heater were made with 0.065-mm copper wires. The cases of the two carbon-glass resistors were each soldered to a small 0.7-mm diameter gold wire with Woods metal. The resistor leads were thermally anchored to the gold wire before they were soldered to 0.1-mm diameter manganin wires. These manganin wires, which were thermally anchored to the heat sink at their other ends, ensured electrical contact to the sensors with negligible heat losses because of their poor thermal conductance. The gold wires were clamped lightly to the sample, and then varnished. The distance between these wires, L, could not be estimated to better than $\sim$15%, which is the limiting factor to the absolute accuracy of our measurements. The heat sink was kept stable in temperature to a few mK. Below the liquid-helium boiling point, this temperature stability was achieved by pumping on the bath and regulating the pressure; above 4.2 K we used a capacitance temperature controller. The sample was in an isothermal copper can, evacuated to about 10^{-4} Torr. For each value of field and sink

temperature, the temperatures at the sensor positions $T_H(0)$ and $T_C(0)$ defined in Fig. 1 were measured when no heat was applied. The nominal values of $T_C(0)$ and $T_H(0)$, computed using the in-field calibration tables,[13] were within $\sim 2\%$ of each other up to 15 T, thus verifying the applicability of these tables. To improve the accuracy of our measurements, however, this small error in temperature reading was further reduced to a second-order error by using Eq. (3) below.

A constant thermal power Q was then applied (see Fig. 1) and $T_H(Q)$ and $T_C(Q)$ were measured after temperature equilibrium was achieved. The temperature differences $[T_H(Q)-T_C(Q)]$ were kept smaller than one-tenth of the absolute temperature. The thermal conductivity was then calculated as

$$\kappa = \frac{Q(L/S)}{[T_H(Q)-T_H(0)]-[T_C(Q)-T_C(0)]} , \tag{3}$$

where L is the distance between the probes, and S the cross section of our samples. The sample cross section was constant to $\lesssim 1\%$ over the distance L. For the small temperature differences used in this experiment, the linearization of the heat equation given above is valid; furthermore the validity of this relation was checked experimentally by variation of the heat current. The average sample temperature corresponding to each thermal conductivity point determined from Eq. (3) is

$$T_a = \frac{[T_H(Q)+T_C(Q)]}{2} . \tag{4}$$

The accuracy for our measured temperature difference [denominator of Eq. (3)] is better than 3% at 15 tesla. Some of the experimental points shown below in the $\kappa(T)$ plots were reproduced by taking different combinations of $T_H(Q)$ and $T_C(Q)$ to yield the same T_a values. Because of the magnetoresistance of the strain-gauge heater resistor, it was not possible to keep T_a constant during the magnetic field sweeps. Thus, after choosing a fixed T_a we measured κ at two different average temperatures, one slightly above T_a and the other slightly below T_a. We then determined κ at T_a by interpolating between the two sets of experimental points.

The scatter of the experimental points (by about 5%) in the field or temperature sweeps can be seen on the curves shown below. Finally the heat losses are mainly associated with the copper wires leading to the heater. These losses could not be estimated from the thermal conductivity of the copper wires, because we did not know the exact temperature gradient across the wires. Since we could not calculate the losses, we estimated them experimentally by measuring the apparent conductance of a glass microscope slide which is assumed to have zero conductance because glass has poor thermal conductivity, and we used a long, thin sample. The heat losses follow a linear T^1 law, and are approximately given by $0.18\times 10^{-3}T$ (W/K) at zero field. The heat losses are expected to be smaller at high field because of the magnetoresistance of copper. In view of the geometrical S/L factor of our samples, the heat losses in the wires and contacts contribute an error of less than 4% to any of the thermal conductivity measurements reported here.

The samples of size $\sim 4\times 16\times 1$ mm^3 were prepared using the two-zone method in which the intercalant vapor is kept at a lower temperature than the graphite host.[14] The staging conditions were determined by the temperature difference between the graphite and the vapor. After intercalation, the x-ray stage determination showed the stage-5 potassium sample to contain less than 10% admixture of other stages. For the more dilute compounds the x-ray stage determination can only be regarded as approximate because the line shifts are comparable to the linewidths. Furthermore, since the sample thickness (between 1 and 2 mm) is large compared to the x-ray penetration depth, the x-ray stage characterization does not guarantee that the sample is well staged throughout the bulk, which contributes to the thermal conductivity.

Precautions were taken during the sample mounting procedures to prevent desorption of the intercalant. X-ray characterization of the sample after the thermal-conductivity experiment had been completed indicated that the stage was preserved during the experiment.

III. RESULTS

The aim of the present work is to separate the thermal conductivity of GIC samples into their lattice (κ_L) and electronic (κ_E) contributions, by using a high magnetic field to create a magnetoresistance to deplete κ_E via Eq. (2), and obtain a situation where $\kappa_E(B) \ll \kappa_L$. As each experimental κ versus temperature curve was taken, we checked that this condition is verified by plotting the thermal resistivity κ^{-1} versus field. In the simplest case, the observation of saturation in such a plot

implies that $\kappa^{-1} \cong \kappa_L^{-1}$. For the particular case of bismuth, which has two types of carriers with high mobilities and high partial thermopowers, the situation is more complicated.[10] After we establish for every sample the temperature and field range over which the saturation condition is satisfied, we can determine the temperature dependence of κ and κ_L and hence also of the difference between κ and κ_L which is κ_E.

In this section, we shall first present the results of this procedure on a sample of pristine HOPG. We then show the results on one donor and one acceptor compound for which this separation between κ_L and κ_E was achieved between 4 and 40 K. Finally, for completeness, we also show results on samples for which we could not separate κ_E and κ_L with the magnetic field range that was available.

Figure 2(a) shows the field dependence of the thermal resistivity of the HOPG sample which was used as the host material for the intercalation compounds measured in this work. Holland *et al.*[11] previously reported saturation of $\kappa^{-1}(B)$ below a field of 1 T, which we observed here too. The small decrease in thermal resistivity at high field in Fig. 2(a) is probably due to an irreproducibility in the magnetoresistance of the temperature sensors,

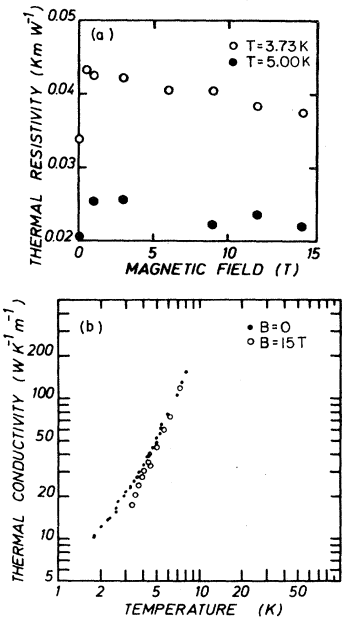

FIG. 2. (a) Magnetic field dependence at the indicated average sample temperatures of the thermal resistivity for a sample of the pristine HOPG used as host material for the intercalation compounds. (b) Temperature dependence of the thermal conductivity for the same sample at zero field and 15 T.

and is well within the accuracy range claimed for the calibration of the sensors.[13]

The temperature dependence of the thermal conductivity of the HOPG sample used in the present work is shown in Fig. 2(b). The zero-field plot (solid circles) shows a $T^{2.4}$ temperature law at high temperatures, with a decreasing exponent in the temperature law at low temperatures. At a field of 15 T (open circles), the $T^{2.4}$ law persists to lower temperatures, quite consistently with the experiments of Ref. 10.

The following figures report the results of the temperature dependence of κ with and without a magnetic field performed on different stages of graphite intercalated with donor or acceptor species. The results for the field dependence of the thermal resistivity of a stage-$\sim$7 potassium sample are shown in Fig. 3(a) for various temperatures, and it is seen that saturation is achieved for $T \gtrsim 4$ K for the available field range. It is observed experimentally that saturation does not occur for the available field range for $T < 4$ K. Figure 3(b) shows the temperature dependence of κ in zero field and at 13 T; the high-field curve hence represents the lattice thermal conductivity κ_L of this sample. The difference between $\kappa(B=0)$ and κ_L gives rise to the solid curve, which in view of Eq. (1), we call κ_E, the electronic thermal conductivity at low temperatures. From the figure we see that for this dilute donor compound κ_E increases with a linear T^1 law at low temperatures and gradually saturates at higher temperatures, similar to the behavior for κ_E in most impure metals.[15] Since saturation of the thermal-conductivity curves in Fig. 3(a) is not achieved below $\sim$4 K, the curve labeled κ_E may be an overestimate for the electronic contributions for $T \lesssim 4$ K.

Similar results are obtained for a dilute *acceptor* compound, as shown in Fig. 4. The magnetic field dependence of the thermal resistivity $\kappa^{-1}(B)$ is presented in Fig. 4(a) for the dilute $FeCl_3$ compound (approximately stage 9), showing saturation for $T \gtrsim 4$ K. The points in Fig. 4(b) show the temperature dependences of κ at zero field and at 14 T. Since $\kappa(B=14\text{ T}) \simeq \kappa_L$ for $T \gtrsim 4$ K, we can obtain the temperature dependence of the difference between the two curves, designated by κ_E (solid curve). In this case the low-temperature power law for κ_E is T^1 but after a maximum is reached in the (10–20)-K range, κ_E begins to fall off. The fall off in κ_E is not observed for the stage-$\sim$7 potassium sample in Fig. 3(b).

Figure 5(a) shows the field dependence of κ^{-1} in a $FeCl_3$ stage-5 compound for $T=7.06$ K. Since

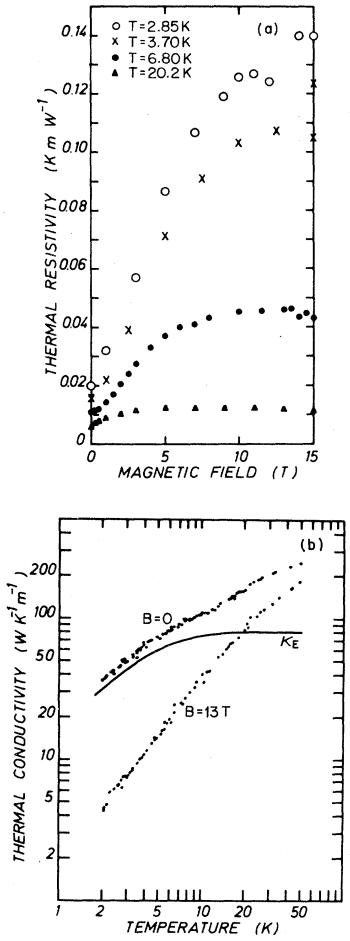

FIG. 3. (a) Magnetic field dependence at the indicated average sample temperatures of the thermal resistivity for a stage-$\sim$7 potassium-graphite compound. (b) Temperature dependence of the thermal conductivity for the same sample as in (a) at zero field and 13 T. For most of the temperature range, the high-field data in (b) represent the lattice thermal conductivity. Difference between the low-field and high-field data is given by the solid curve, which represents the electronic thermal conductivity.

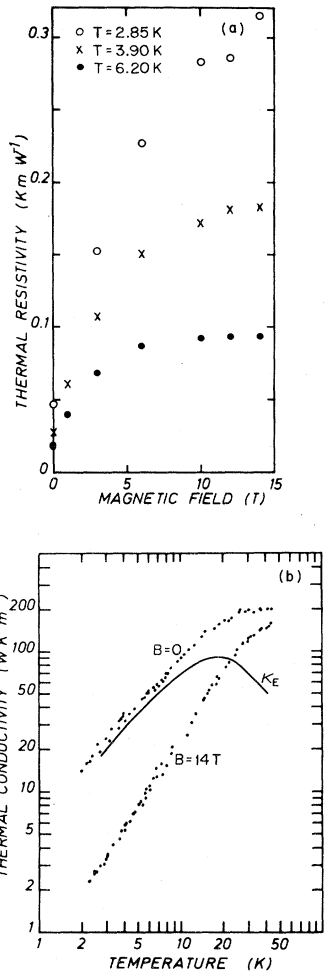

FIG. 4. (a) Magnetic field dependence at the indicated average sample temperature of the thermal resistivity for a dilute (stage-$\sim$9) $FeCl_3$ graphite compound. (b) Temperature dependence of the thermal conductivity for the same sample as in (a) at zero field and 14 T. For $T > 3$ K, the high-field points in (b) represent the lattice thermal conductivity. Solid curve represents the difference between the zero-field and high-field data, and is identified with the electronic thermal conductivity (see text).

this curve almost saturates by 15 T, one expects, in analogy with all the other samples measured in this work, that the electronic contribution is quenched near $B = 15$ T for temperatures $T > 8$ K. Using these results, we plot in Fig. 5(b) the temperature dependent $\kappa(T)$ at zero field and at 15 T, for $T < 13$ K. We can only report the separation of κ into κ_L and κ_E for the temperature range $8 < T < 13$ K. We could not extend our field measurements to higher temperatures because the Bitter magnet exploded during the measurements, destroying the sample.

Figure 6 shows the field dependence of the thermal resistivity of a stage-5 potassium-intercalated sample. No saturation behavior could be clearly identified below 18 K; hence the separation of κ_L and κ_E could not be achieved over a large enough temperature range at the highest available magnetic field to obtain κ_E.

IV. DISCUSSION

A. The electronic transport

The data on the electronic thermal conductivity of our compounds can be used together with the

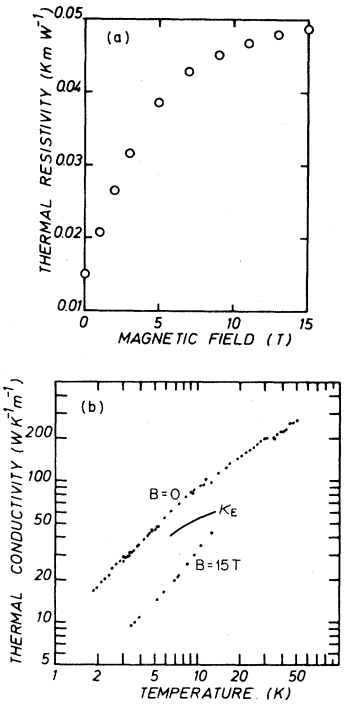

FIG. 5. (a) Magnetic field dependence of the thermal resistivity of a stage-5 $FeCl_3$ graphite compound at an average temperature of 7.06 K. (b) Thermal conductivity of the same sample vs temperature at zero field and 15 T. High-field points represent, for $T > 7$ K, the lattice thermal conductivity. The solid curve gives the difference between the zero-field and high-field data, and is identified with the electronic thermal conductivity over the narrow temperature range ($8 < T < 13$ K).

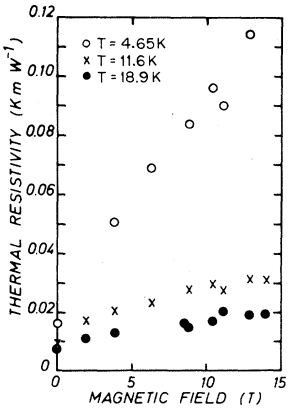

FIG. 6. Magnetic field dependence of the thermal resistivity of a stage-5 potassium-intercalated graphite sample for the indicated average temperatures. No saturation behavior could be clearly identified for the available magnetic field range.

Wiedemann-Franz law, Eq. (2), and the free-electron value L_0 to give results for the electrical resistivity ρ of our samples as a function of temperature. The results are presented in Fig. 7, and we estimate this temperature dependence of ρ to be accurate to $\pm 8\%$ (see Sec. III). The Wiedemann-Franz law is expected to hold only when elastic or quasielastic electron scattering is assumed. This is usually the case when impurities are the dominant scatterers, or for large-angle electron-phonon scattering.[15]

Both the donor and acceptor compounds show a temperature-independent resistivity at the lowest temperatures; this is presumably the residual resistivity range where electron impurity scattering dominates. This region extends to a higher temperature for the acceptor (15 K) than for the donor (2.5 K) compound. The resistivity data for the potassium-intercalated sample are consistent with those of Ref. 16 where a linear T^1 temperature dependence is reported at higher temperatures. The dilute $FeCl_3$ compound displays a T^2 dependence of resistivity for $T \gtrsim 20$ K.

We now use the results in Fig. 7 to estimate the temperature dependence of the mobility μ. If we assume a one-carrier-type model where the electrical conductivity is given by

$$\sigma = Ne\mu \,, \tag{6}$$

in which N is the carrier density, we can estimate the temperature dependence of the average carrier mobility. Since the charge carrier density is much larger than that for graphite for all samples that were measured, the sample is expected to be metal-

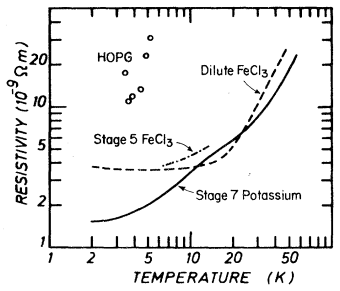

FIG. 7. Temperature dependence of the electrical resistivity of HOPG, of a stage-5 $FeCl_3$-intercalated compound, of a dilute $FeCl_3$-intercalated compound, and of a stage-$\sim$7 potassium-intercalated compound. These resistivities are obtained by applying the Wiedemann-Franz law [Eq. (2)] to the observed electronic thermal conductivity, i.e., the difference between the zero-field and high-field experimental thermal conductivities.

TABLE I. Values for the stoichiometric ratio ξ, the charge transfer coefficient f_X, and the carrier density N estimated using Eq. (7). Estimates were made using commonly quoted values for ξ ($\xi=12$ for K and $\xi=6.6$ for $FeCl_3$) and for d_s, the intercalate sandwich thickness ($d_s=5.35$ Å for K and $d_s=9.42$ Å for $FeCl_3$) (see Ref. 24).

Intercalant	Stage	I_c (Å)	ξ	f_X	N (cm^{-3})
HOPG[a]	∞	3.35			5.5×10^{18}
K	5	18.75	12	1	1.71×10^{21}
K	~7	25.45	12	1	1.26×10^{21}
$FeCl_3$	5	22.82	6.6	0.2[b]	5.10×10^{20}
$FeCl_3$	~9	36.22	6.6	0.2[b]	3.22×10^{20}

[a]From Ref. 17. For HOPG we have taken I_c as the interlayer graphite distance, neglecting the *AB* stacking of the graphite layers.
[b]From Ref. 24.

lic, with a temperature-independent carrier density. The carrier density is estimated from the charge transfer per intercalant f_X by

$$N=\frac{N_C}{n\xi}f_X\frac{nc_0}{I_c}\ , \tag{7}$$

and the values for N pertinent to the various samples investigated in this work are given in Table I. In Eq. (7), $N_C=1.15\times10^{23}$ cm^{-3} is the density of carbon atoms, n is the stage, ξ is the stoichiometric ratio in the chemical formula $C_{n\xi}X$, c_0 is the interplanar carbon distance ($c_0=3.35$ Å), and I_c is the c-axis repeat distance of the intercalation compound. In making this estimate for N we have made use of the relation $I_c=(n-1)c_0+d_s$, where d_s is the distance between two graphite layers between which the intercalant is sandwiched.

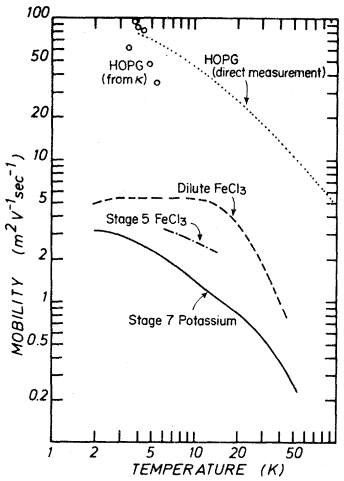

FIG. 8. Average carrier mobility vs temperature for the same samples as in Fig. 7. These mobilities are obtained from the resistivities of Fig. 7 and the carrier densities summarized in Table I. The dotted line shows, for comparison, the temperature dependence of the mobility of a good-quality HOPG sample measured directly (Ref. 17).

The mobility of the HOPG sample near 4 K, as determined from analysis of the thermal-conductivity measurements using the Wiedemann-Franz relation, is within the range of values for good-quality HOPG samples as measured directly[17] and shown by the dotted curve in Fig. 8. This confirms the validity of our analysis. The stage-~7 potassium GIC reported here has a mobility that is a factor of 3 higher than the highest value previously reported for any potassium GIC,[14] but the mobility for the stage-~7 compound is still far lower than that for HOPG. Both of our $FeCl_3$ intercalated samples have mobilities that are yet higher, in agreement with previous results on donors and acceptors, which are compared in Ref. 14. However, for the donor compound, μ is still increasing with decreasing T below 4 K, which indicates that electron-phonon scattering is important in this range. From the temperature independence of the low-temperature mobility, we conclude that the acceptor compound has its charge carriers scattered predominantly by impurities up to 15 K. (The stage dependence of electron-impurity scattering near 4 K will be more extensively discussed for acceptor compounds in Ref. 18.) The phonons thus seem less effective scatterers in the acceptor compound than in the donor compound. It is also interesting that the temperature power law seems larger in the acceptor compound ($\sim T^2$) than in the donor ($\sim T^1$); this indicates that small-angle scattering occurs with higher probability in acceptors than in donors. (In the small-angle scattering regime, the Wiedemann-Franz law may break down.[15])

These conclusions about the scattering processes

TABLE II. Values for a and b that fit the data in Figs. 2(b), 3(b), and 4(b) to the power law $\kappa_L = aT^b$.

Intercalant	Stage	Temperature region of validity (K)	a (W/K m)	b
HOPG	∞	$3 < T < 8$	1	2.4
K	~ 7	$3 < T < 15$	1.64	1.3
$FeCl_3$	~ 9	$3 < T < 25$	0.58	1.6

are consistent with the known properties of phonons and electrons in GIC's. These low-temperature thermal-conductivity results imply that $FeCl_3$ intercalation creates more damage to the graphite lattice than intercalation with K. A similar behavior has also been reported for the intercalation of K and $FeCl_3$ into certain graphite fibers based on the analysis of their Raman spectra.[19] Furthermore, despite the fact that in donor compounds the Fermi surfaces are larger than in acceptor compounds, the donor compounds have a larger density of low-frequency phonons with flat dispersion curves.[20] This means that for these donor compounds, even at low temperatures (~ 4 K), there are large-momentum phonons available to scatter electrons from one side of the Fermi surface to the other.

B. The lattice thermal conductivity

The present thermal-conductivity experiments imply that most of the lattice conduction is via the graphite planes: Indeed our samples are dilute, and graphite itself has a very high thermal conductivity compared to most materials. Since rather little has been reported about properties such as the Debye cutoff frequency or velocity of sound for the in-plane direction of the graphite layers in GIC's, we use in our interpretation of the thermal-conductivity measurements the corresponding data for pure graphite which are known.

Although we shall not attempt to explain the lattice thermal conductivity in detail, we can comment on two properties exhibited by the experimental curves: the prevalent temperature power law, and the magnitude of the lattice contribution.

We approximate the experimental κ_L by a law

$$\kappa_L = aT^b \tag{8}$$

in the temperature region where this dependence applies and values of a and b are given in Table II for all the samples that were measured. The results show that the power law for our pristine graphite HOPG material ($b = 2.4$) falls within the limits for b obtained by other workers ($b = 2.5 \pm 0.2$) for pure HOPG samples of high perfection.[7,21] Using the model for thermal conductivity developed in Ref. 21, the phonons in our sample would have a mean free path of ~ 30 μm at 10 K, compared to 10 μm for de Combarieu's sample[22] and 4.5 μm for that of Holland *et al.*[11]

The fact that in intercalated samples both the power law and the magnitude of κ_L are greatly reduced is consistent with observations in the low-temperature thermal conductivity of neutron-irradiated graphite[22] for which a $T^{1.5}$ law for κ was observed. Dreyfus and Maynard[23] interpreted the results of Ref. 22 and attributed the $T^{1.5}$ law to irradiation-induced defects.

The phonon mean free path in the intercalated samples appears to be reduced by 1 to 2 orders of magnitude with respect to pure graphite. A more complete model for the phonon thermal conductivity, based on Ref. 21 and what is known about the nature of the defects,[14] is needed to give a quantitative interpretation of the present results on κ_L.

ACKNOWLEDGMENTS

The authors wish to thank Dr. G. Dresselhaus for many fruitful discussions, P. Coopmans for construction of the cryostat, Dr. L. Rubin and Dr. B. Brandt and their staff at the Francis Bitter National Magnet Laboratory for technical assistance and advice, and L. Salamanca-Riba for help with the experiments. The authors also acknowledge Air Force Office of Scientific Research Contract No. F49620-81-C-0006 for support of the research. The HOPG material was kindly provided by Dr. A. W. Moore of Union Carbide. Two of us (J.H. and M.S.) were visitors at the Francis Bitter National Magnet Laboratory which is supported by the NSF. Also, one of us (J.H.) was supported by Fonds National Belge de la Recherche Scientifique.

[1]B. T. Kelly, A. Whittaker, D. Tobin, and P. Wagner, Carbon 9, 447 (1971).
[2]J. Boxus, B. Poulaert, J-P. Issi, H. Mazurek, and M. S. Dresselhaus, Solid State Commun. 38, 1117 (1981).
[3]J. Heremans, J-P. Issi, I. Zabala-Martinez, M. Shayegan, and M. S. Dresselhaus, Phys. Lett. 84A, 387 (1981).
[4]B. Poulaert, J. Heremans, J-P. Issi, I. Zabala-Martinez, H. Mazurek, and M. S. Dresselhaus, Extended Abstracts of the 15th Biennial Conference on Carbon, Philadelphia, 1981, edited by W. C. Forsman, p. 92.
[5]B. T. Kelly, in *Chemistry and Physics of Carbon,* edited by P. L. Walker (Dekker, New York, 1969), Vol. 5, p. 119.
[6]C. N. Hooker, A. R. Ubbelohde, and D. A. Young, Proc. R. Soc. London Ser. A 276, 83 (1963).
[7]B. T. Kelly and K. E. Gilchrist, Carbon 7, 355 (1969).
[8]J-P. Issi, J. Heremans, G. Dresselhaus, and M. S. Dresselhaus, in *Proceedings of the 4th International Conference on the Physics of Narrow Gap Semiconductors, Linz, 1981,* edited by E. Gornik, H. Heinrich, and L. Palmetshofer (Springer, Berlin, 1982), p. 363.
[9]L. L. Sparks, Adv. Cryo. Eng. 24, 224 (1978).
[10]C. Uher and H. J. Goldsmid, Phys. Status Solidi B 65, 765 (1974).
[11]M. G. Holland, C. A. Klein, and W. D. Straub, J. Phys. Chem. Solids 27, 903 (1966).
[12]J-P. Issi, J. Boxus, B. Poulaert, and J. Heremans, in *Proceedings of the 17th International Conference on Thermal Conductivity, 1981* (in press).
[13]H. Sample, B. L. Brandt, and L. Rubin, Rev. Sci. Instrum. (in press).
[14]M. S. Dresselhaus and G. Dresselhaus, Adv. Phys. 30, 139 (1981).
[15]R. Berman, *Thermal Conduction in Solids* (Clarendon, Oxford, 1976).
[16]D. G. Onn, G. M. T. Foley, and J. E. Fischer, Phys. Rev. B 19, 6474 (1979).
[17]I. L. Spain, in *Chemistry and Physics of Carbon,* edited by P. L. Walker (Dekker, New York, 1973), Vol. 8, p. 1.
[18]J-P. Issi, J. Heremans, I. Zabala-Martinez, and M. S. Dresselhaus (unpublished).
[19]P. Kwizera, M. S. Dresselhaus, and G. Dresselhaus, in Ref. 4, p. 100, and Carbon (in press).
[20]J. Giergiel, P. C. Eklund, R. Al-Jishi, and G. Dresselhaus (unpublished).
[21]B. T. Kelly, Carbon 6, 71 (1968).
[22]A. de Combarieu, J. Phys. (Paris) 28, 951 (1967).
[23]B. Dreyfus and R. Maynard, J. Phys. (Paris) 28, 955 (1967).
[24]T. Krapchev, R. Ogilvie, and M. S. Dresselhaus, Carbon (in press).